LncRNA SNHG16 promotes epithelial-mesenchymal transition by upregulating ITGA6 through miR-488 inhibition in osteosarcoma

Jie Bu [a,*], Ru Guo [b], Xue-Zheng Xu [a], Yi Luo [a], Jian-Fan Liu [a]

[a] Department of Orthopaedics, Hunan Cancer Hospital and The Affiliated Cancer Hospital of Xiangya School of Medicine, Central South University, Changsha 410013, Hunan Province, People's Republic of China
[b] Department of Pediatrics, Maternal and Child Health Care Hospital of Hunan Province, Changsha 410008, Hunan Province, People's Republic of China

ARTICLE INFO

ABSTRACT

Background: Osteosarcoma is a primary cause of cancer-associated death in children and adolescents worldwide. Long non-coding RNAs SNHG16 (lncRNA SNHG16) and integrin subunit-a 6 (ITGA6) are recently reported to be involved in the tumorigenesis of osteosarcoma by multiple mechanisms. However, the correlation between SNHG16 and ITGA6 in osteosarcoma remains undetermined.
Methods: Expression of miR-488, SNHG16 and ITGA6, as well as epithelial-mesenchymal transition (EMT) associated markers in osteosarcoma tissues and cell lines were examined by qRT-PCR or Western blotting. Effects of miR-488, SNHG16 and ITGA6 on cell migration, invasion were evaluated by wound-healing assay and transwell assay. Bioinformatics analysis and dual-luciferase reported assays were applied to assess the interaction among miR-488, SNHG16 and ITGA6. RNA immunoprecipitation (RIP) was also used to verify SNHG16 and miR-488 interaction. Finally, animal study was used to detect the effect of SNHG16 on osteosarcoma *in vivo*.
Results: SNHG16 and ITGA6 were significantly increased while miR-488 was decreased in osteosarcoma. ITGA6 was screened as a target gene of miR-488, and SNHG16 was sponged by miR-488 in osteosarcoma cells. MiR-488 overexpression and SNHG16 knockdown suppressed migration, invasion and EMT of osteosarcoma cells. Moreover, rescue assays proved that the influences of SNHG16 on osteosarcoma cells migration, invasion and EMT were dependent on miR-488 and ITGA6. In addition, the promotive effects of SNHG16 on osteosarcoma tumor growth and metastasis were further supported by xenograft tumor growth assay.
Conclusion: SNHG16 promoted migration, invasion and EMT of osteosarcoma by sponging miR-488 to release ITGA6.

1. Background

Osteosarcoma, characterized by high incidence in teenagers and young adults, is the most common histological subtype of primary bone tumor, accounting for more than 56% of all bone tumors [1]. Approximately six in every million teenagers and two in every million adults will be diagnosed as osteosarcoma [2]. Osteosarcoma cells usually shows high metastatic potential with approximately 20% of osteosarcoma patients presenting with metastases [3]. Osteosarcoma cells could metastasize to multiple human tissues and organs, of which the lung is the most common site to metastasize [4]. The five-year survival rate of osteosarcoma patients with localized lesion is approximately between 65% and 70%, however, the number drops to 19% and 30% in those patients with distant metastasis [5,6]. Traditional therapeutic strategy for newly diagnosed osteosarcoma rely mainly on the combination of surgical resection and chemotherapy [3,7]. Although the combinative therapy improves the prognosis of osteosarcoma patients in a certain extent, its therapeutic effects were recently reported to be seriously limited by drug-resistance of osteosarcoma [8,9]. To improve prognosis of osteosarcoma patients, novel strategies targeting the molecular basis of osteosarcoma are essential.

It is well known that less than two percent of transcripts of the human genome possess protein-encoding capacity, while most of

the rest lack of the ability of encoding protein and be term as non-coding RNAs (ncRNAs) [10,11]. MicroRNAs (miRNAs, with approximately 22 nucleotides) is an important member of ncRNAs [12,13]. Abnormal expression profiles of miRNAs were frequently observed in osteosarcoma, indicating that it might involve in the pathogenesis of osteosarcoma [14]. Wang et al., has reported that miR-486 suppressed the osteosarcoma cell invasion and epithelial-mesenchymal-transition (EMT) through targeting PIM1 [15]. Moreover, miR-126 was demonstrated to suppress proliferation, migration, invasion and EMT process of osteosarcoma cells via targeting ZEB1 [16]. Increasing evidences have shown that miR-488 might act as a tumor suppressor in various human tumors, such as colorectal cancer [17] and hepatocellular carcinoma [18]. In gastric cancer, overexpression of miR-488 suppressed cell proliferation, colony information and migration [19]. In tongue squamous cells, miR-488 was revealed to inhibit invasion and EMT by targeting ATF3 [20]. Furthermore, miR-488 was reported to be downregulated in osteosarcoma by a miRNAs signatures analysis [21]. As a well-demonstrated tumor suppressor, miR-488 has been revealed to inhibit the progression of osteosarcoma by Jing Qiu et al., in 2018 [22]. However, the role of miR-488 in EMT of osteosarcoma has remained largely unclear. An amount of evidences have shown that miRNAs could bind and regulate their target genes, thereby exhibiting their biological functions in cancers. MiR-488 was also revealed to target various of genes, such as ATF3, HMGN5 and ADAM9 [18,20,23]. Herein, ITGA6 was screened to be a new target gene of miR-488. ITGA6 could be targeted by miR-127-3p, thereby involved in the pathogenesis of osteosarcoma. These findings implied that miR-488 might participate in the regulation of EMT of osteosarcoma via ITGA6.

According to the competitive endogenous RNA (ceRNA) theory, lncRNAs could competitively bind to miRNAs via miRNA response elements, thereby modulating corresponding genes at posttranscriptional level [10,20,24]. Long non-coding RNAs (lncRNAs, with over 200 nucleotides), another important member of ncRNAs, have been reported to be correlated with numerous human diseases [25]. The lncRNA small nucleolar RNA host gene 16 (SNHG16) was previously demonstrated to regulate the tumorigenesis of multiple tumors, including lung, colorectal and breast cancer, and it was also revealed to be dysregulated in osteosarcoma, recently [21,26]. Su et al., have reported that SNHG16 promoted osteosarcoma cell invasion and migration, by sponging miR-340 [27]. SNHG16 was reported to facilitate osteosarcoma progression and attenuated cisplatin sensitivity by interacting with miR-16/ATG4B axis; moreover, the ectopic expression of SNHG16 was found to be closely correlated with poor prognosis and lower overall survival rate [28,29]. However, whether SNHG16 promoted EMT by sponging miR-488 has still unknown. By using starBase database, we found that SNHG16 had putative binding sites for miR-488. In view of the oncogenic or repressive effects of SNHG16 or miR-488 in osteosarcoma, and the potential interaction between them, we proposed that SNHG16 might participate in the EMT process of osteosarcoma by regulating ITGA6 through miR-488.

In the present study, SNHG16/miR-488/ITGA6 axis was demonstrated to regulate the EMT process in osteosarcoma, implying that SNHG16, miR-488 and ITGA6 might be potential biomarkers for osteosarcoma diagnosis and treatment.

2. Methods

2.1. Tissues collection and cell lines

Ten pairs of osteosarcoma and adjacent normal tissues were gathered in the present study from osteosarcoma patients who were diagnosed at Hunan Cancer Hospital between 2015 and 2018. Tissue samples were stored at -80 °C until experiment. Tissue collection and manipulates were approved by the Ethics Committee of the Hunan Cancer Hospital. Informed consents were collected from all participants.

Two osteosarcoma cell lines (U2OS and HOS) were provided by the Cell Bank of the China Science Academy, Shanghai. Cells were growth at 37 °C under 5% CO_2 in the RPMI-1640 medium (Gibco Laboratories, Grand Island, NY), which supplemented with 10% fetal bovine serum (Gibco) and 1% penicillin/streptomycin.

2.2. Cell morphology assay

For the examination of the morphology change during EMT process, treated U2OS and HOS cells were collected and seeded into 24-well plates at a concentration of 2×10^6 cells per well. The cell morphology was monitored by an inverted microscope (Axiovert 10 ZEISS).

2.3. Quantitative real-time PCR (qRT-PCR)

RNAs of osteosarcoma tissues and cells were prepared with TRIzol reagent (Invitrogen, Carlsbad, CA, USA) after 48 h of transfection. Then, extracted total RNAs (2 µg) were reverse-transcribed into cDNA using a PrimeScript first stand cDNA Synthesis Kit (Takara, Japan). PCR amplification was conducted with a Maxima SYBR Green qPCR Master Mix kit (Thermo Fisher Scientific, MA) on the ABI Prism 7700 sequence detection system (PE Applied Biosystems, California, USA). Sequence of primers used in this study was showed in Table 1, and the expression of each gene was calculated according to the $2^{-\Delta\Delta CT}$ method. PCR reactions were run in triplicate in three independent experiments.

2.4. Oligonucleotides transfection

SNHG16 short hairpin RNA (sh-SNHG16) and its negative control (sh-NC), miR-488 mimics, miR-488 inhibitor and its negative control (NC), and ITGA6-overexpressing plasmid (OE-ITGA) were all designed and purchased from Vigenebio (Shanghai, China). For transfection, osteosarcoma cells were maintained in culture medium at 37 °C for 16 h (when cells were grown to 70–80% confluence), and then transfected with oligonucleotides by using Lipofectamine 3000 (Invitrogen, Carlsbad, CA, USA) following the protocols of manufacturers. Cells were collected for RNA and protein isolation 48 h after transfection.

2.5. CCK-8 assay

Treated osteosarcoma cells were seeded into 96-well plates at 4000 cells/well. After 8 h of culture at 37 °C, 10 µL of Cell Counting Kit-8 solution (CCK-8/WST-8; Sigma) was added into each well and incubated for another 2 h. Afterwards, the absorbance of each plate was examined at 450 nm.

2.6. Wound-healing assay

After 48 h of transfection, osteosarcoma cells were collected and re-suspended with cultured medium at a density of 2×10^4 cells/mL. Subsequently, cell suspensions were seeded into 6-well plates and cultured at 37 °C until 80% confluence. A sterile pipette tip was used to scratch the culture surface, and the wound closure was examined after 24 h and 48 h to assess the migration of osteosarcoma cells.

Table 1
The primer forward and primer reverse for qRT-PCR.

Gene	Primer forward (5′–3′)	Primer reverse (5′–3′)
MIR100HG	CACTGGTCTGCCCTTCCTAA	GGGGATGAACCATTGACAAC
miR-488	CGGCCGTTGAAAGGCTATTTC	GTCGTATCCAGTGCAGGGTCCGAGGTATTCGCACTGGATACGACGACCAA
ITGA6	GGGAGTACCTTGGTGGATCA	AGCATGGATCTCAGCCTTGT
E-cadherin	TCACATCCTACACTGCCCAG	AGTGTCCCTGTTCCAGTAGC
N-cadherin	GAGTTAAGGCGCCATCCTCA	AGCACTGCCACCTGGAAAAT
Vimentin	GGACCAGCTAACCAACGACA	AAGGTCAAGACGTGCCAGAG
Snail	AATCGGAAGCCTAACTACAGCG	GTCCCAGATGAGCATTGGCA
GAPDH	CCAGGTGGTCTCCTCTGA	GCTGTAGCCAAATCGTTGT

2.7. Transwell assay

The migratory and invasive capacities of osteosarcoma cells were evaluated by transwell chambers (Corning Incorporated, USA) with and without Matrigel matrix (BD Biosciences, USA), respectively. Briefly, 24 h after transfected with corresponding oligonucleotides, osteosarcoma cells (2×10^4 cells/mL) were collected and re-suspended with culture medium (serum free). Subsequently, 500 μL serum free cell suspension and 200 μL FBS-supplemented culture medium were added into upper and lower chamber, respectively. After incubating at 37 °C for 48 h, osteosarcoma cells passed into lower chamber were fixed with 4% paraformaldehyde, followed by staining with 0.1% crystal violet for 30 min. Six random fields of every group under microscope were photographed and counted.

2.8. Western blot assay

After 48 h of transfection with corresponding oligonucleotides, osteosarcoma cells were collected and lysed with the RIPA buffer (Bio-Rad, CA, USA). Total proteins of treated osteosarcoma cell lysis were extracted and its concentration was determined by a BCA kit (Pierce, USA) according to the procedures obtained from the manufacturers. Total proteins (50 μg) were loaded into and isolated with 10% SDS-PAGE. Target proteins were next transferred into the PVDF membranes (Millipore, Bedfordshire, UK) and incubated with 5% skimmed milk for 2 h to block non-specific binding sites. Then, the membranes were incubated with primary antibodies that against GAPDH (1:10,000, ab181602, abcam, UK); E-cadherin (1:500, ab15148, abcam, UK), N-cadherin (1:2000, ab18203, abcam, UK), Vimentin (1:1000, ab92547, abcam, UK), Snail (1:1000, ab82846, abcam, UK) and ITGA6 (1:50, ab75737, abcam, UK) overnight. After washing twice with PBS, the membranes were incubated with horseradish peroxidase conjugated corresponding secondary antibodies (IgG-HRP, Abcam, 1:2000, UK) for 2 h, and signals were detected through the enhanced chemiluminescent reagents (ECL, Germany). Intensity of bands was analyzed by Quantity One software (Bio-Rad, USA), and results were normalized to the intensity of GAPDH.

2.9. Dual-luciferase reporter assay

The fragments of ITGA6 and SNHG16 including miR-488 target sites were amplified and sub-cloned into the plasmids pmirGLO vectors (Promega, Madison, WI) to establish the pmir-ITGA6-WT and pmir-SNHG16-WT recombinant reporter vectors. The mutant miR-488 binding sites of ITGA6 and SNHG16 were also amplified and inserted into the plasmids pmirGLO vectors to construct the pmir-ITGA6-MUT and pmir-SNHG16-MUT recombinant reporter vectors. Osteosarcoma cells were plated into 24-well plates and maintained for 48 h, then, the miRNAs (miR-488 mimics and mimics NC) and the recombinant reporters (WT or MUT) were co-transfected into osteosarcoma cells and maintained at 37 °C for

another 48 h. Finally, the transfected osteosarcoma cells were collected to examine the relative luciferase intensity.

2.10. RNA immunoprecipitation (RIP) assay

Correlation between SNHG16 and miR-488 was verified via EZ-Magna RIP RNA-binding protein immunoprecipitation kit (Millipore) following the procedure of manufacturers. In brief, osteosarcoma cells transfected with miR-488 mimics were lysed with RIP lysis buffer, and 200 μL cell lysate was subjected to the incubation with RIP immunoprecipitation buffer containing magnetic beads that conjugated with human anti-Argonaute2 (Ago2) antibody (Millipore). Normal mouse IgG (Millipore) was applied as negative control. The enrichment of SNHG16 and PVT1 (positive control) was tested through qRT-PCR.

2.11. Xenograft tumor growth and in vivo metastasis evaluation

Ten-weeks BALB/c mice (male) were provided by National Laboratory Animal Center (Beijing, China), and animals treatments were approved by Animal Care Committee of Central South University. Mice were kept in pathogen-free environment with free access to food and water. To obtain stable SNHG16-knockdown cell lines, lentiviral particles were produced by HEK293T cells co-transfected with sh-SNHG16 and psPAX2 and pMD2.G plasmids. Next, osteosarcoma cells were infected with lentiviral particles in the presence of polybrene (8 μg/ml, Genechem, China). After 5 days, puromycin-resistant cells were collected and examined using qRT-PCR. Then, stable SNHG16-knockdown osteosarcoma cells (1×10^6) were inoculated into the back of mice. Tumor volume was examined every 7 days and then was weighted after 35 days of inoculation. Tumor volume was measured using the formula: length $\times$ (width)^2 $\times$ 1/2.

For *in vivo* metastasis assessment, transfected osteosarcoma cells (1×10^6) were injected into mice through tail vein. After 35 days of inoculation, these animals were sacrificed and lung tissues were collected for metastatic nodules analysis using HE staining.

2.12. Hematoxylin and eosin (HE) staining

Briefly, tumors were collected and fixed in 4% paraformaldehyde. After fixation, tissues were embedded with paraffin and sliced into 5 μm sections, then, followed by HE staining using a Hematoxylin and Eosin kit (ab245880, abcam, UK) following the instructions of manufacturers.

2.13. Data analysis

Experimental data was expressed as mean ± standard deviation (SD). Statistical analysis was conducted in GraphPad Prism 7.0 via student's *t* test (two groups comparison) or one-way analysis of

variance (multiple groups comparison), followed by Tukey post hoc test. P less than 0.05 was considered to be significance.

3. Results

3.1. Different expression of SNHG16, miR-488 and ITGA6 in osteosarcoma

Multiple genes associated with the pathogenesis of osteosarcoma were identified to be target by miR-488, including TGIF2, ITGA6, CDK6, E2F3, and IGF2BP3. We examined the expression of TGIF2, ITGA6, CDK6, E2F3, and IGF2BP3 in osteosarcoma cells transfected with miR-488 mimics and inhibitor by qRT-PCR. As results indicated that miR-488 mimic transfection caused a significant downregulation of ITGA6 in osteosarcoma cells, and ITGA6 expression level exhibited the biggest alteration among the dysregulated genes (Fig. S1A). Inhibition of miR-488 resulted in a remarkable upregulation of ITGA6 in osteosarcoma cells, and ITGA6 also exhibited the biggest alteration among the dysregulated genes (Fig. S1B). Thus, ITGA6 was selected for further study. To evaluate the roles of SNHG16, miR-488 and ITGA6 on osteosarcoma, relative expression levels of SNHG16, miR-488 and ITGA6 were examined by qRT-PCR in osteosarcoma and normal tissues. According to the results of qRT-PCR, SNHG16 and ITGA6 were significantly increased while miR-488 was remarkably reduced in osteosarcoma tissues compared to normal ones (Fig. 1A–C), implying that SNHG16, miR-488 and ITGA6 might has a key role in the osteosarcoma pathogenesis.
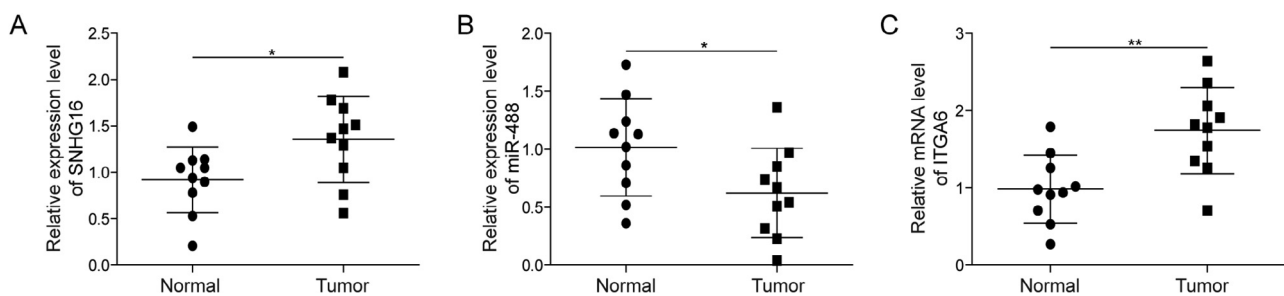
3.2. MiR-488 suppressed osteosarcoma cell migration, invasion and EMT

Influences of miR-488 on osteosarcoma cell migration, invasion and EMT were evaluated in miR-488 mimics treated U2OS and HOS cells using wound-healing, transwell assay and EMT-related gene detection. Overexpression efficiency of miR-488 in U2OS and HOS cells were verified by qRT-PCR (Fig. 2A). Functionally, as suggested by wound-healing assay, U2OS and HOS cells showed decreased migratory capacity after taransfected with miR-488 mimics (Fig. 2B). Meanwhile, transwell assay demonstrated that U2OS and HOS cells showed decreased migratory and invasive capacity after miR-488 overexpression (Fig. 2C and 2D). In addition, overexpression of miR-488 could also increase the cell viability of U2OS and HOS (Fig. S1E). EMT was considered to be a fundamental process of tumor cell migration and invasion. We thus assessed the effects of miR-488 overexpression on EMT process of osteosarcoma cells by detecting the expression of EMT-related gene E-cadherin, N-cadherin, Vimentin and Snail. Results from qRT-PCR and Western blot assays showed that miR-488 overexpression in U2OS and HOS cells resulted in increased mRNA and protein levels of E-cadherin and reduced expression of N-cadherin, Vimentin and Snail (Fig. 2E and F). These findings suggested that miR-488 overexpression in vitro inhibited osteosarcoma cell migration, invasion and EMT.

3.3. Overexpression of ITGA6 abolished the inhibitory influences of miR-488 on osteosarcoma cells migration, invasion and EMT

To investigate the underlying mechanisms, we screened the target gene of miR-488 through bioinformatics measures, results showed that ITGA6 might be targeted by miR-488 (Fig. 3A). The interaction between miR-488 and ITGA6 was confirmed by dual-luciferase reporter assay in U2OS and HOS cells. Treatment of miR-488 mimics reduced the luciferase intensity of U2OS and HOS cells driven by ITGA6 WT, but not ITGA6 MUT (Fig. 3B). Subsequently, ITGA6 expression was detected in miR-488 overexpressed or silenced osteosarcoma cells by qRT-PCR and Western blot assays. Efficiency of miR-488 knockdown in U2OS and HOS cells was determined by qRT-PCR (Fig. 3C). Relative mRNA expression of ITGA6 was significantly decreased in miR-488 mimics treated U2OS and HOS cells while it was remarkably increased in miR-488 inhibitor treated U2OS and HOS cells (Fig. 3C). Western blot analysis exhibited a marked reduction of ITGA6 protein in miR-488 mimics treated U2OS and HOS cells and a significant upregulation of ITGA6 protein in miR-488 inhibitor treated U2OS and HOS cells (Fig. 3D). These results suggested that miR-488 negatively regulated the expression of ITGA6 by directly sponging ITGA6. We then further evaluated the effects of ITGA6 on miR-488 induced inhibition of migration, invasion and EMT of osteosarcoma cells by treating U2OS and HOS cells with miR-488 mimics plus ITGA6. Wound-healing assay showed that the inhibitory effects of miR-488 on migration were blocked by ITGA6 (Fig. 3E). The miR-488 overexpression induced migration and invasion inhibition was also reversed by ITGA6 (Fig. 3F and G). Results from CCK-8 assay indicated that the inhibitory effects of miR-488 on cell proliferation were abolished by the treatment of ITGA6 simultaneously (Fig. S1D). In addition, results from qRT-PCR and Western blot assays showed that ITGA6 treatment could reverse the miR-488 induced upregulation of E-cadherin and downregulation of N-cadherin, Vimentin and Snail (Fig. 4A and B). Moreover, cells in the non-transfected and mimic NC groups displayed a mesenchymal-like phenotype, while those cells in miR-488 mimic group exhibited an epithelial-like phenotype, indicating that miR-488 overexpression inhibited EMT (Fig. S2A). However, co-transfection of miR-488 and ITGA6 reversed the EMT inhibition by miR-488 (Fig. S2A). These results indicated that ITGA6 might act as a downstream gene of miR-488 in osteosarcoma, and miR-488 could inhibit the EMT of osteosarcoma cells via restraining ITGA6 expression.


Fig. 1. Different expression of SNHG16, miR-488 and ITGA6 in osteosarcoma. Expression levels of SNHG16 (A), miR-488 (B) and ITGA6 (C) in osteosarcoma and normal tissues were evaluated by qRT-PCR. *P < 0.05, **P < 0.01, ***P < 0.001. Difference between groups was analyzed using student's *t* test.
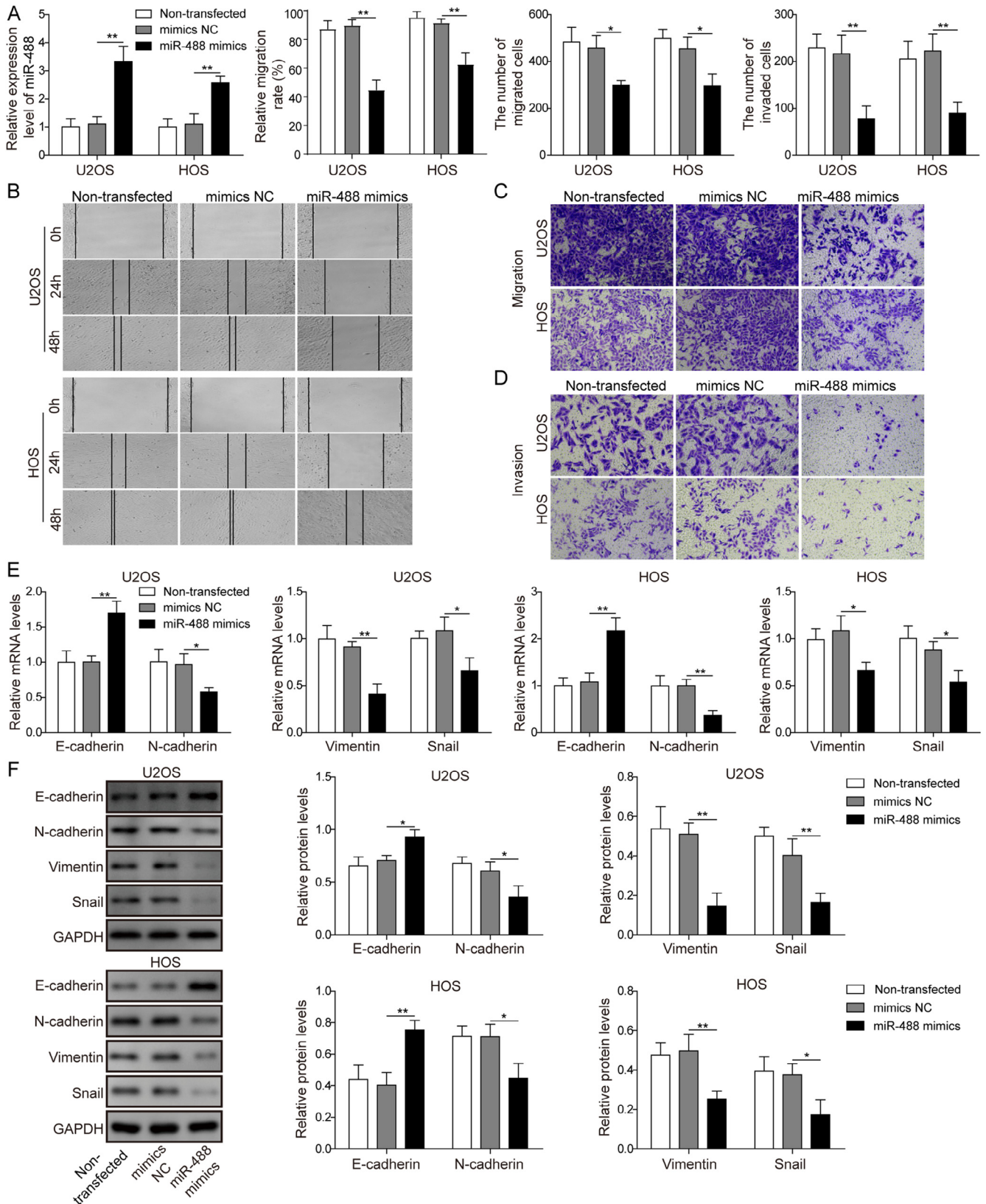
Fig. 2. MiR-488 inhibited migration, invasion and EMT of osteosarcoma cells. (A) After treating with miR-488 mimics, miR-488 expression of U2OS and HOS cells was detected by qRT-PCR. (B and C) Wound-healing assay and transwell assay were performed to examine cell migration of U2OS and HOS cells treated with miR-488 mimics. (D) Influences of miR-488 overexpression on U2OS and HOS cell invasion were assessed in through transwell assay. The mRNA and protein expression levels of E-cadherin, N-cadherin, Vimentin and Snail in U2OS and HOS cells transfected with miR-488 mimics were determined by (E) qRT-PCR and (F) Western blotting, respectively, error bars showed mean ± SD, N = 3, *P < 0.05, **P < 0.01, ***P < 0.001. Difference between groups was analyzed using one-way analysis of variance.
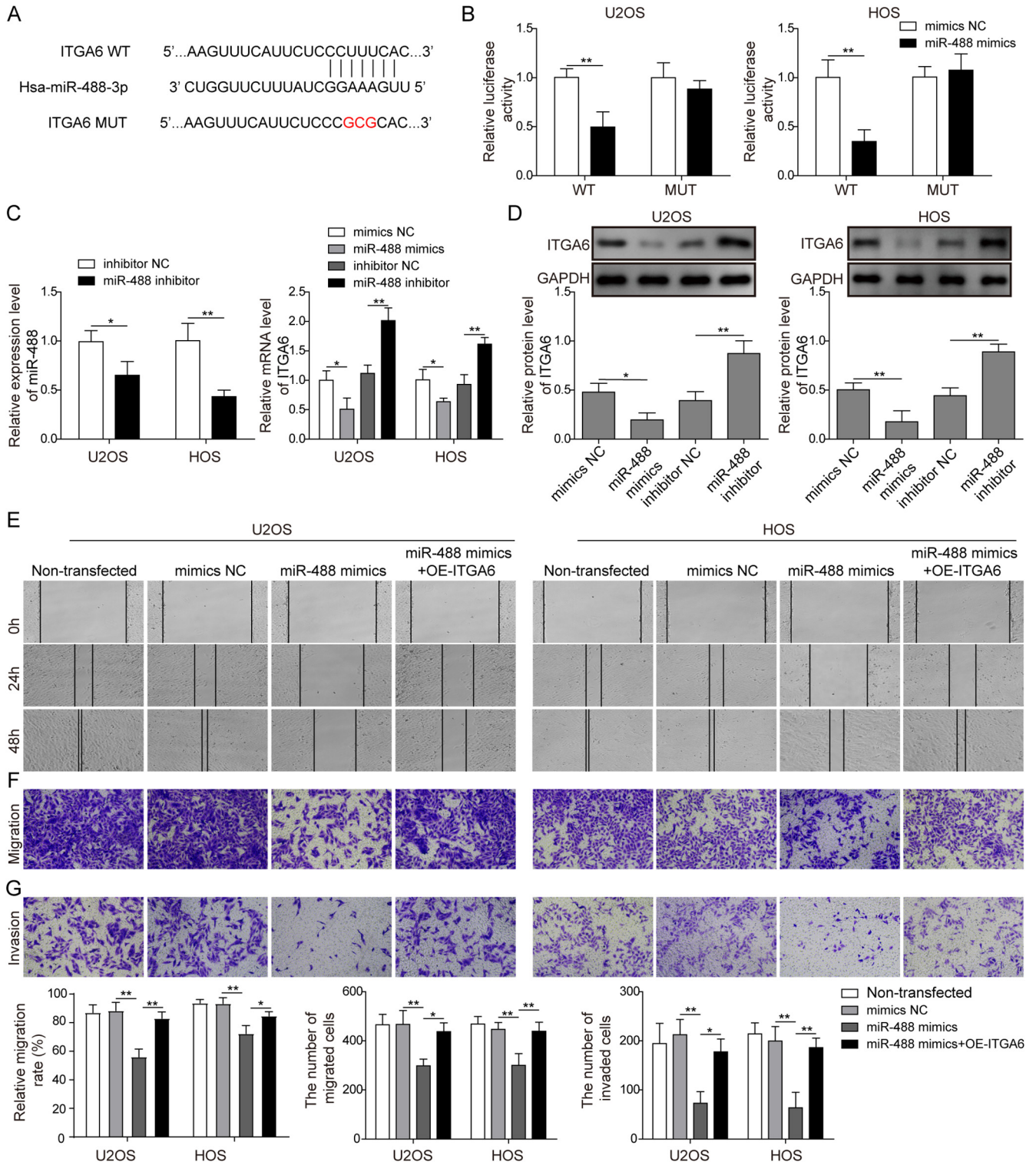
Fig. 3. Overexpression of ITGA6 abolished the inhibitory effects of miR-488 on migration and invasion. (A) Sequence of target site between miR-488 and ITGA6. (B) Interaction between miR-488 and ITGA6 was verified by dual-luciferase reporter assay. (C) Expression of miR-488 was detected by qRT-PCR in U2OS and HOS cells transfected with miR-488 inhibitor; relative mRNA expression of ITGA6 of U2OS and HOS cells transfected with miR-488 mimics or inhibitor was measured by qRT-PCR. (D) Western blot analysis was carried out to test the influences of miR-488 overexpression and knockdown on ITGA6 expression of U2OS and HOS cells. (E) Wound-healing and (F and G) transwell assays were performed to evaluate the effects of ITGA6 overexpression on cell migration and invasion in miR-488 overexpressed U2OS and HOS cells, error bars showed mean ± SD, N = 3, $^*P < 0.05$, $^{**}P < 0.01$, $^{***}P < 0.001$. Difference between groups was analyzed using student's t test (two groups comparison) or one-way analysis of variance (multiple groups comparison).
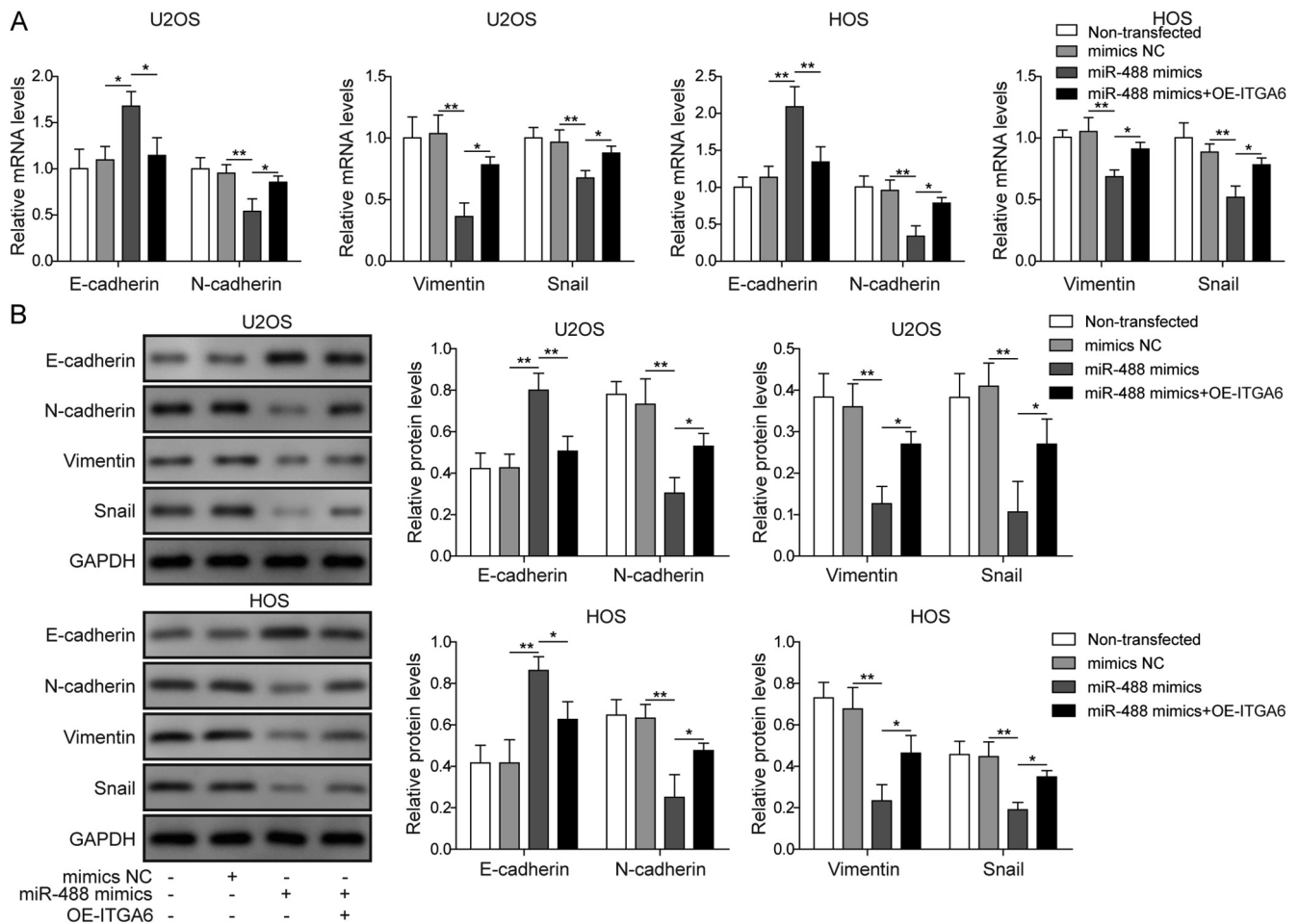
Fig. 4. Overexpression of ITGA6 abolished the inhibitory effects of miR-488 on EMT of osteosarcoma cells. (A) qRT-PCR and (B) Western blot assays were carried out in miR-488 overexpressed U2OS and HOS cells to assess the effects of ITGA6 overexpression on the expression of E-cadherin, N-cadherin, Vimentin and Snail, error bars showed mean ± SD, N = 3, *P < 0.05, **P < 0.01, ***P < 0.001. Difference between groups was analyzed using one-way analysis of variance.
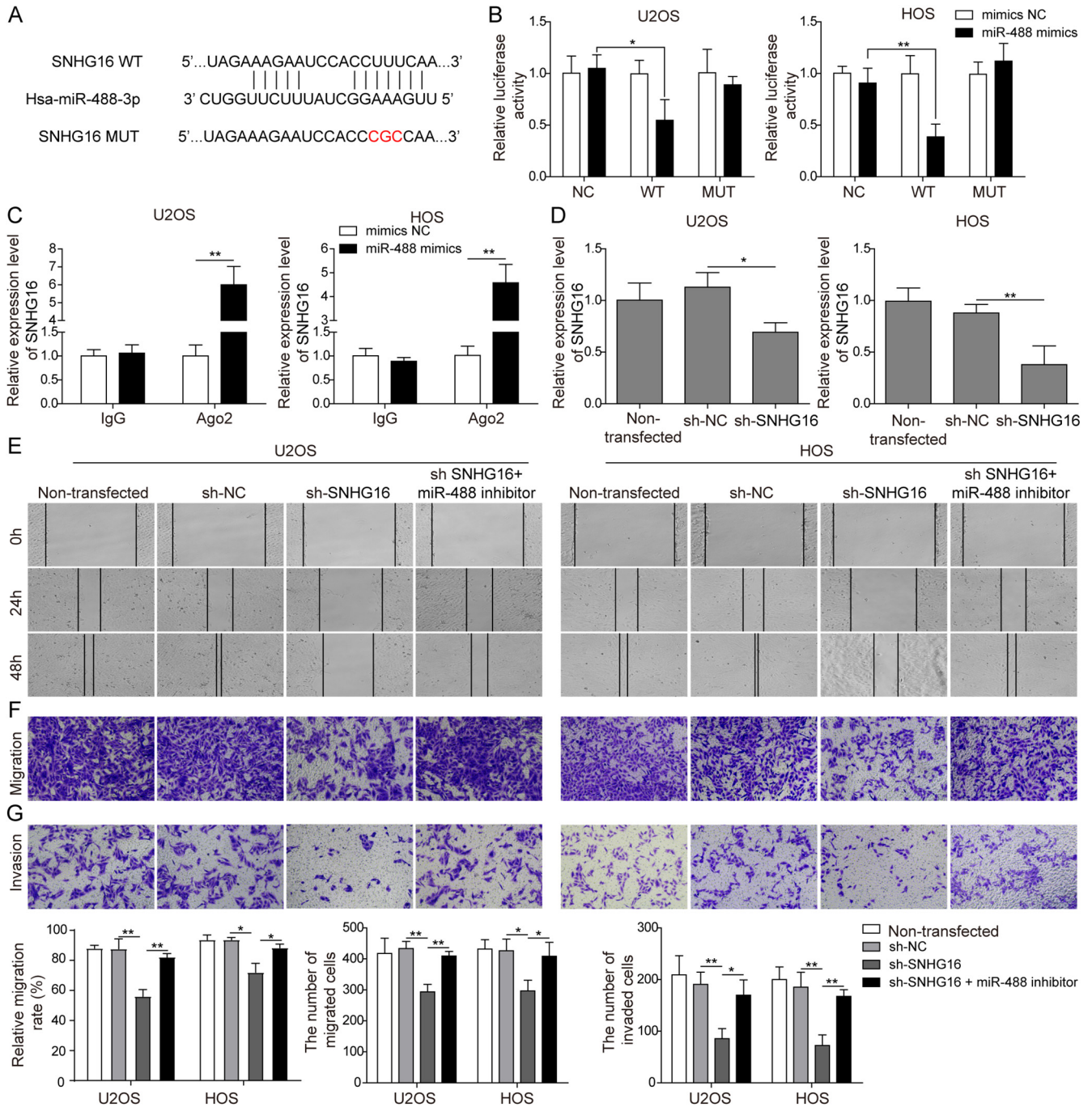
3.4. SNHG16 promoted osteosarcoma cells migration, invasion and EMT by sponging miR-488

Moreover, bioinformatics measures indicated that miR-488 could be sponged by SNHG16 (Fig. 5A). Dual-luciferase reporter assay was carried out to test the correlation between miR-488 and SNHG16. Results suggested that miR-488 mimics reduced the luciferase intensity of U2OS and HOS cells driven by SNHG16-WT, but not SNHG16-MUT, compared to mimics NC treatment (Fig. 5B). We then adopted anti-Ago2 RIP assay in U2OS cells transiently overexpressing miR-488. To validate the pulldown of Ago2 in miR-488 media is functioning, lncRNA-PVT1, a well demonstrated target lncRNA of miR-488, was used as positive control in RIP assay. As results indicated that PVT1 was enriched in U2OS and HOS cells transfected with miR-488 mimics (Fig. S1C). Endogenous SNHG16 pull-down was also specifically enriched in miR-488 transfected U2OS and HOS cells (Fig. 5C), indicating that miR-488 was sponged by SNHG16. These results implied that SNHG16 physically interacted with miR-488 in osteosarcoma cells. We then further investigated the influences of SNHG16 knockdown on migration, invasion and EMT in miR-488 inhibitor treated U2OS and HOS cells. Relative SNHG16 expression in sh-SNHG16 treated U2OS and HOS cells was evaluated by qRT-PCR analysis. Results showed that sh-SNHG16 treatment significantly decreased the expression of SNHG16 in U2OS and HOS cells compared to sh-NC treatment (Fig. 5D). Wound-healing and tranwell assays in U2OS and HOS cells showed that sh-SNHG16 significantly suppressed

cell migration and invasion, while sh-SNHG16 and miR-488 inhibitor simultaneously treatment significantly reversed the suppressive influences of sh-SNHG16 on cell migratory and invasive abilities (Fig. 5E–G). By using CCK-8 assay, we revealed that the repressive effects of sh-SNHG16 on cell proliferation of U2OS and HOS cells were reversed by the co-transfection of sh-SNHG16 and miR-488 inhibitor (Fig. S1D). Furthermore, in the qRT-PCR and Western blot detection, sh-SNHG16 was demonstrated to evidently enhance E-cadherin while decrease N-cadherin, Vimentin and Snail of U2OS and HOS cells; these effects of sh-SNHG16 could also be blocked by the co-treatment of sh-SNHG16 and miR-488 inhibitor (Fig. 6A and B). The promotive effects of SNHG16 on EMT was supported by the cell morphology change examination, knockdown SNHG16 in osteosarcoma cells exhibited epithelial-like phenotype and co-treatment of sh-SNHG16 and miR-488 inhibitor reversed the morphology change induced by sh-SNHG16 (Fig. S2B). These findings suggested that SNHG16/miR-488 axis has a critical role in the osteosarcoma cell migration, invasion and EMT.

3.5. ITGA6 overexpression abrogated the influences of SNHG16 knockdown on osteosarcoma cells migration, invasion and EMT

Based on the above, miR-488 inhibitor could reverse the suppressive influences of sh-SNHG16 on proliferation, migration, invasion and EMT of osteosarcoma cells, we then tested whether ITGA6 involved in the influences of sh-SNHG16. We treated U2OS and

Fig. 5. SNHG16 promoted migration and invasion of osteosarcoma cells by sponging miR-488. (A) Sequence of binding site between SNHG16 and miR-488. Interaction between SNHG16 and miR-488 was tested by (B) dual-luciferase reporter and (C) RIP assay. (D) Knockdown efficiency of sh-SNHG16 in U2OS and HOS cells was determined by qRT-PCR. Effects of miR-488 inhibition on (E and F) cell migration and (G) invasion were evaluated by wound-healing and transwell assays in sh-SNHG16 treated U2OS and HOS cells, error bars showed mean ± SD, N = 3, *P < 0.05, **P < 0.01, ***P < 0.001. Difference between groups was analyzed using student's *t* test (two groups comparison) or one-way analysis of variance (multiple groups comparison).

HOS cells with sh-NC, sh-SNHG16 and sh-SNHG16 + OE-ITGA6. The data showed that sh-SNHG16 + OE-ITGA6 remarkably reversed the inhibitory influences of sh-SNHG16 on proliferation (Fig. S1C), migration (Fig. 7A and B) and invasion (Fig. 7C) of U2OS and HOS cells. Moreover, we examined the EMT-related gene expression levels (E-cadherin, N-cadherin, Vimentin and Snail) in sh-NC, sh-SNHG16 and sh-SNHG16 + OE-ITGA6 transfected U2OS and HOS cells by qRT-PCR and Western blot assays. Compared to sh-SNHG16 group, sh-SNHG16 + OE-ITGA6 treatment significantly

inversed the effects of sh-SNHG16 on the increase of E-cadherin, and decrease of N-cadherin, Vimentin and Snail (Fig. 7D and E). The promotive effects of SNHG16 on EMT was supported by the cell morphology change examination, knockdown of SNHG16 osteosarcoma cells exhibited epithelial-like phenotype and overexpression of ITGA6 was also revealed to abolish the morphology change induced by sh-SNHG16 (Fig. S2B). Taken together, ITGA6 might be indirectly regulated by SNHG16, thereby regulated osteosarcoma cell migration, invasion and EMT.
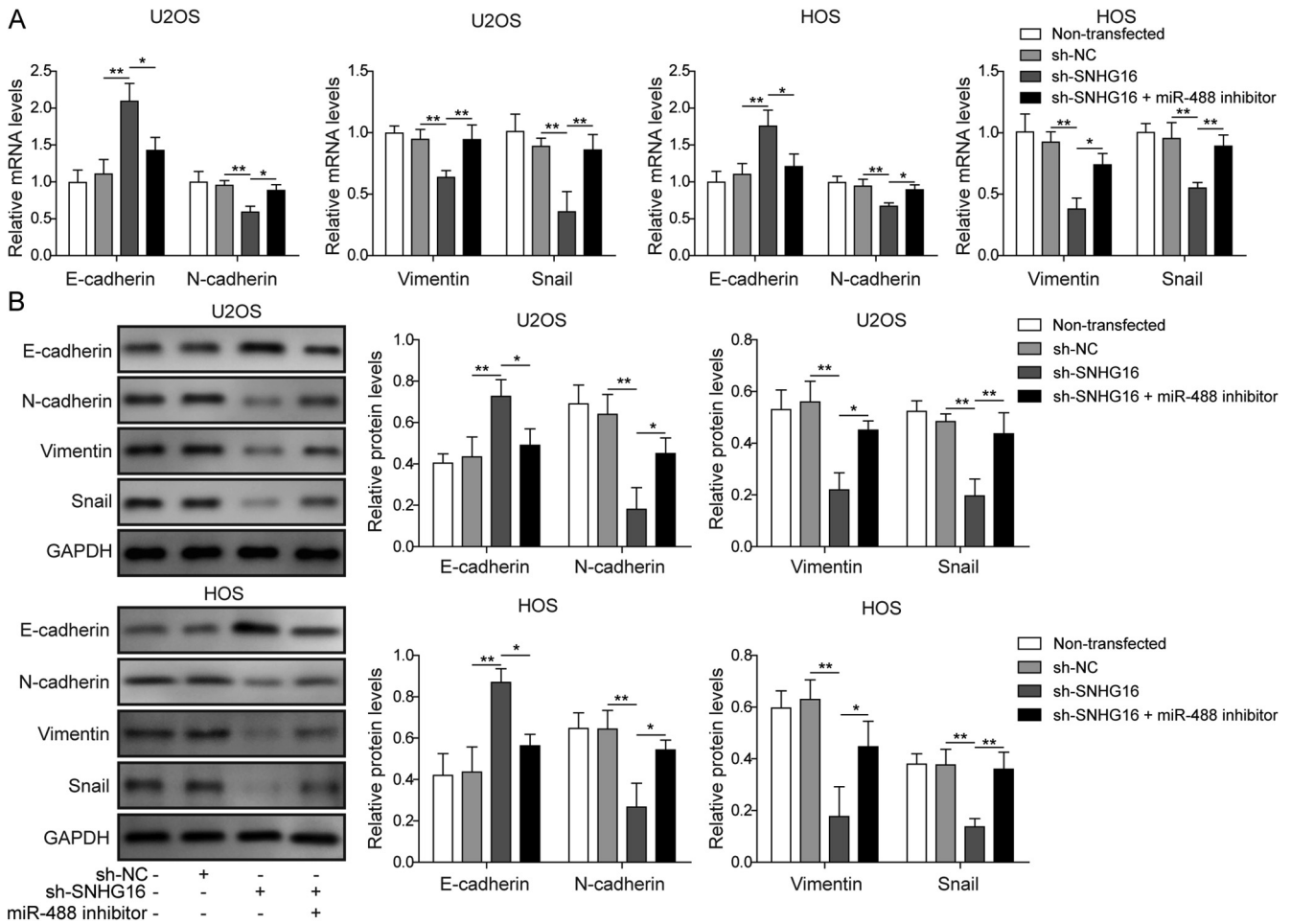
Fig. 6. SNHG16 promoted EMT of osteosarcoma cells by sponging miR-488. (A and B) Influences of miR-488 inhibition on the expression of E-cadherin, N-cadherin, Vimentin and Snail were assessed via qRT-PCR and Western blot analysis in SNHG16 blocked U2OS and HOS cells, error bars showed mean ± SD, N = 3, *P < 0.05, **P < 0.01, ***P < 0.001. Difference between groups was analyzed using one-way analysis of variance.

### 3.6. Knockdown of SNHG16 repressed osteosarcoma tumor growth in vivo

To further evaluate the functions and mechanisms of SNHG16 in osteosarcoma *in vivo*, we inoculated the sh-NC and sh-SNHG16 transfected osteosarcoma cells into the left flank of nude mice. After 35 days of inoculation, tumors were isolated and examined (Fig. 8A). The volume of tumors from sh-SNHG16 group was significantly decreased compared to that from sh-NC group (Fig. 8A). Tumor weight of sh-SNHG16 group was dramatically reduced compared to that of sh-NC group (Fig. 8A). Next, qRT-PCR was adopted to examine the expression levels of SNHG16, miR-488 and ITGA6 in the xenograft tumors. As results indicated that SNHG16 and ITGA6 were remarkably downregulated while miR-488 was remarkably upregulated in sh-SNHG16 group compared to that in sh-NC group (Fig. 8B). Moreover, by using Western blotting, we found E-cadherin was significantly increased while N-cadherin, Vimentin and Snail were significantly decreased in sh-SNHG16 group compared to that in sh-NC group (Fig. 8C). To examine the effects of SNHG16 knockdown on tumor metastasis *in vivo*, we observed the metastatic nodules of lung after invocation of sh-NC and sh-SNHG16 transfected osteosarcoma cells through tail vein injection. As results showed that the metastatic nodules of lung were markedly decreased in sh-SNHG16 group compared to that in sh-NC group (Fig. 8D). Histopathologic analysis of lung tissue further supported this conclusion (Fig. 8E). Thus, knockdown

of SNHG16 repressed osteosarcoma tumor growth and metastasis *in vivo*.

4. Discussion

Despite various of comprehensive therapies were applied in the clinical treatment of osteosarcoma, the morbidity and prognosis of osteosarcoma remain dismal [30]. A considerable number of osteosarcoma patients eventually died from complications related to pulmonary metastasis [31]. It is essential to identify the molecular mechanisms of osteosarcoma for the explore of novel diagnostic and therapeutic targets of osteosarcoma.

In this study, we found that SNHG16 and ITGA6 were significantly increased in osteosarcoma tissues, while miR-488 was remarkably decreased compared with adjacent normal tissues. It suggested SNHG16, miR-488 and ITGA6 might played a key role in osteosarcoma. Previous studies have shown that miR-488 acted as a tumor suppressor in multiple human cancers [17,20,32]. The roles of miR-488 in the initiation and progression of multiple human tumors have been well established, however, whether it involved osteosarcoma remain unclear. It was reported that miR-488 was downregulated in osteosarcoma [21]. This study indicated that miR-488 was lowly expressed in osteosarcoma, and overexpression of miR-488 in vitro significantly inhibited osteosarcoma cell migration, invasion and EMT, indicating miR-488 might act
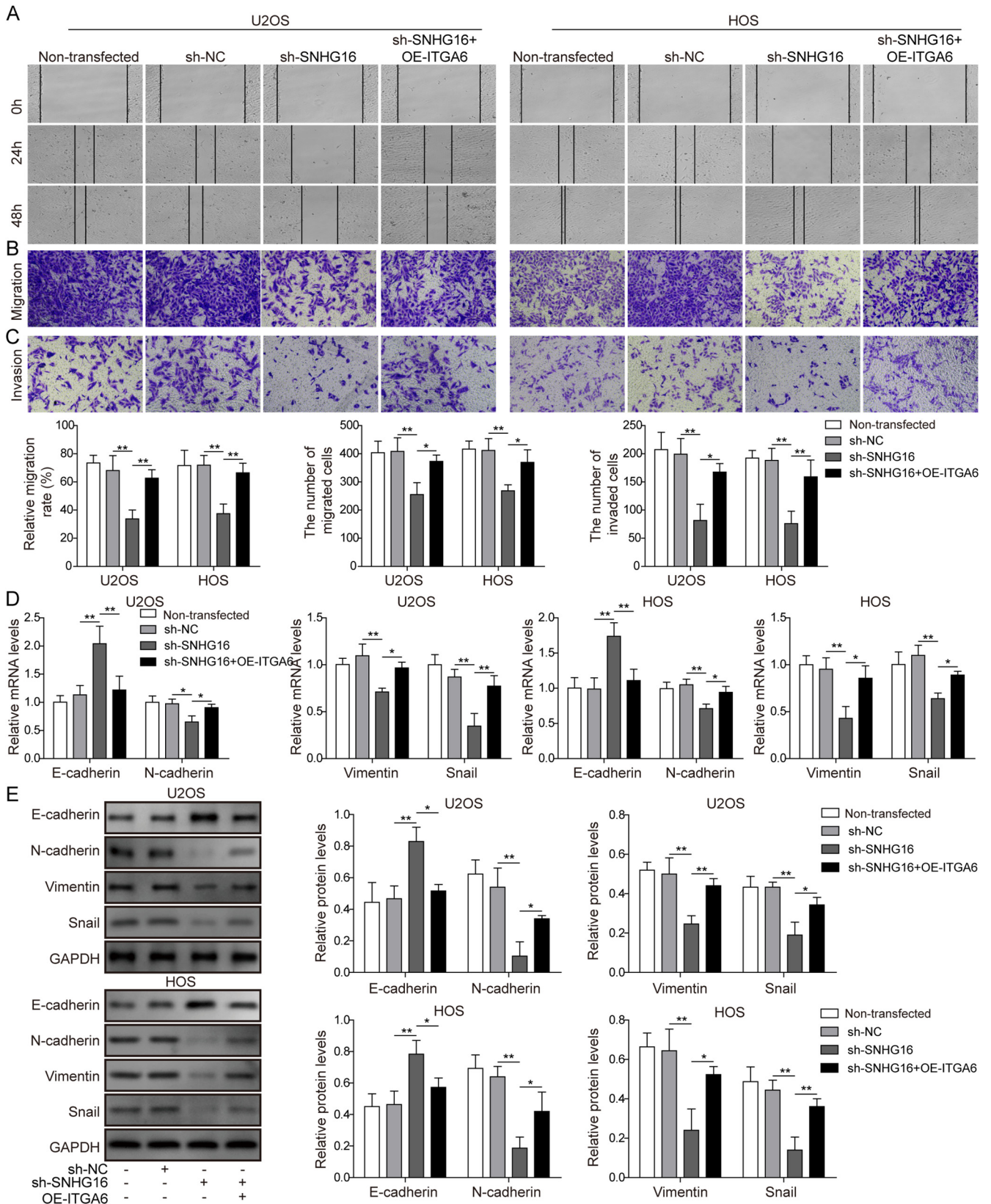
Fig. 7. ITGA6 overexpression reversed the promotive effects of SNHG16 on migration, invasion and EMT of osteosarcoma cells. Effects of ITGA6 overexpression on (A and B) cell migration and (C) invasion were evaluated by wound-healing and transwell assays in SNHG16 blocked U2OS and HOS cells. (D and E) Effects of ITGA6 overexpression on the expression of E-cadherin, N-cadherin, Vimentin and Snail were assessed through qRT-PCR and Western blotting in SNHG16 blocked U2OS and HOS cells, error bars showed mean ± SD, N = 3, *P < 0.05, **P < 0.01, ***P < 0.001. Difference between groups was analyzed using one-way analysis of variance.
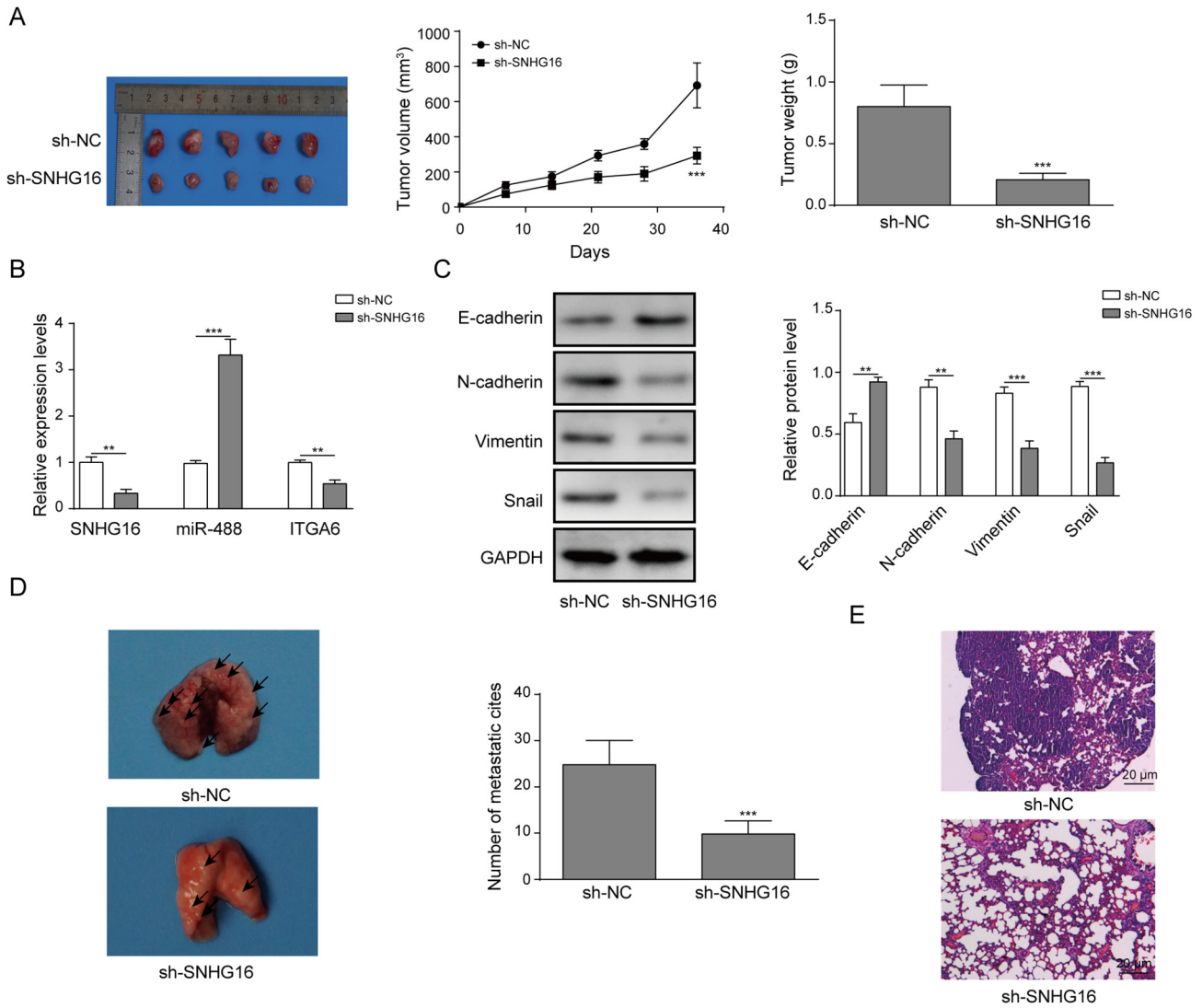
Fig. 8. Knockdown of SNHG16 repressed osteosarcoma tumor growth *in vivo*. (A) Representative images of xenograft tumors derived from sh-NC or sh-SNHG16 transfected osteosarcomacells. Tumor volume was examined every 7 days until 35 days. After 35 days of inoculation, tumors were isolated and weighted. (B) Expression of SNHG16, miR-488, and ITGA6 were detected by qRT-PCR in sh-NC and sh-SNHG16 groups. (C) Protein expression of E-cadherin, N-cadherin, Vimentin and Snail were examined by Western blotting in sh-NC and sh-SNHG16 groups. (D) The metastatic nodules of lung were examined after inoculation of sh-NC and sh-SNHG16 transfected osteosarcomacells through tail vein injection. (E) Histopathological analysis was performed to examined the metastatic nodules of lung in sh-NC and shSNHG16 groups, error bars showed mean ± SD, N = 3, *P < 0.05, **P < 0.01, ***P < 0.001. Difference between groups was analyzed using student's *t* test.

as a tumor suppressor of osteosarcoma. Our finding was consistent with previous reports. ITGA6 was also reported to involve in the regulation of migration, invasion and EMT of various cancer cells [33–35]. In the present study, ITGA6 was identified as a target gene of miR-488 in osteosarcoma cells. Functional assays suggested that overexpression of ITGA6 could abolish the effects of miR-488 mimics on osteosarcoma cell migration, invasion and EMT, which further substantiated that miR-488/ITGA axis plays a critical role in the pathogenesis of osteosarcoma. Taken together, the above evidence demonstrated that miR-488 inhibited the cell invasion, migration and EMT of osteosarcoma by targeting ITGA6.

In addition, our findings also revealed a significant upregulation of SNHG16 in osteosarcoma, and silence of NHG16 resulted in inhibitory effects on osteosarcoma cell invasion, migration and EMT, indicating that SNHG16 acted as an oncogene of osteosarcoma. Most importantly, SNHG16 was predicted to bind with miR-488 in our study, and their interaction was further confirmed by dual-luciferase reporter and RIP assays. Moreover, miR-488 inhibitor and OE-ITGA6 were revealed to reverse the inhibitory effects of SNHG16 knockdown on osteosarcoma cell invasion, migration and

EMT, implying that SNHG16/miR-488/ITGA6 might act as an important regulatory axis in the pathogenesis of osteosarcoma. SNHG16 was previously reported to modulate the invasion, migration and EMT of multiple human tumors [27,36,37]. Recently, Zhu et al., reported that SNHG16 was significantly upregulated in osteosarcoma, and its downregulation resulted in an inhibition of proliferation of osteosarcoma cells [26], which was consistent with our results. Furthermore, the motive effects of SNHG16 on osteosarcoma tumor growth, metastasis and EMT were further supported by the xenograft tumor growth and *in vivo* metastasis assessment. Taken together, these above conclusions suggested that SNHG16/miR-488/ITGA6 axis plays a key role in the tumorigenesis of osteosarcoma.

5. Conclusion

In conclusion, the present work suggested SNHG16/miR-488/ITGA6 axis could regulate the migration, invasion and EMT of osteosarcoma cells, which might be used as potential diagnostic and therapeutic targets for osteosarcoma in the future.

6. Ethics approval

Tissue collection and manipulates were approved by the Ethics Committee of the Hunan Cancer Hospital. Informed consents were collected from all participants. Ten-weeks BALB/c mice (male) were provided by National Laboratory Animal Center (Beijing, China), and animals treatments were approved by Animal Care Committee of Central South University.

CRediT authorship contribution statement

Jie Bu: Conceptualization, Funding acquisition. **Ru Guo:** Writing - original draft, Methodology. **Xue-Zheng Xu:** Data curation, Resources. **Yi Luo:** Formal analysis, Investigation, Software, Visualization. **Jian-Fan Liu:** Project administration, Supervision, Validation, Writing - review & editing.

Declaration of Competing Interest

The authors declare that they have no known competing financial interests or personal relationships that could have appeared to influence the work reported in this paper.

Acknowledgement

Funding

Appendix A. Supplementary data

Supplementary data to this article can be found online at https://doi.org/10.1016/j.jbo.2021.100348.

References

[1] D.D. Moore, H.H. Luu, Osteosarcoma, Cancer Treat. Res. 162 (2014) 65–92.
[2] V.A. Siclari, L. Qin, Targeting the osteosarcoma cancer stem cell, J. Orthop. Surg. Res. 5 (2010) 78.
[3] Y. Zhang, J. Yang, N. Zhao, C. Wang, S. Kamar, Y. Zhou, Z. He, J. Yang, B. Sun, X. Shi, L. Han, Z. Yang, Progress in the chemotherapeutic treatment of osteosarcoma, Oncol. Lett. 16 (5) (2018) 6228–6237.
[4] S. Yu, M.S. Fourman, A. Mahjoub, J.B. Mandell, J.A. Crasto, N.G. Greco, K.R. Weiss, Lung cells support osteosarcoma cell migration and survival, BMC Cancer 17 (1) (2017) 78.
[5] P.A. Meyers, C.L. Schwartz, M. Krailo, E.S. Kleinerman, D. Betcher, M.L. Bernstein, E. Conrad, W. Ferguson, M. Gebhardt, A.M. Goorin, M.B. Harris, J. Healey, A. Huvos, M. Link, J. Montebello, H. Nadel, M. Nieder, J. Sato, G. Siegal, M. Weiner, R. Wells, L. Wold, R. Womer, H. Grier, Osteosarcoma: a randomized, prospective trial of the addition of ifosfamide and/or muramyl tripeptide to cisplatin, doxorubicin, and high-dose methotrexate, J. Clin. Oncol. 23 (9) (2005) 2004–2011.
[6] L. Kager, A. Zoubek, U. Potschger, U. Kastner, S. Flege, B. Kempf-Bielack, D. Branscheid, R. Kotz, M. Salzer-Kuntschik, W. Winkelmann, G. Jundt, H. Kabisch, P. Reichardt, H. Jurgens, H. Gadner, S.S. Bielack, Cooperative German-Austrian-Swiss Osteosarcoma Study, primary metastatic osteosarcoma: presentation and outcome of patients treated on neoadjuvant Cooperative Osteosarcoma Study Group protocols, J. Clin. Oncol. 21 (10) (2003) 2011–2018.
[7] B. Otoukesh, B. Boddouhi, M. Moghtadaei, P. Kaghazian, M. Kaghazian, Novel molecular insights and new therapeutic strategies in osteosarcoma, Cancer Cell. Int. 18 (2018) 158.
[8] Y. Gonzalez-Fernandez, E. Imbuluzqueta, M. Zalacain, F. Mollinedo, A. Patino-Garcia, M.J. Blanco-Prieto, Doxorubicin and edelfosine lipid nanoparticles are effective acting synergistically against drug-resistant osteosarcoma cancer cells, Cancer Lett. 388 (2017) 262–268.
[9] H.K. Brown, M. Tellez-Gabriel, D. Heymann, Cancer stem cells in osteosarcoma, Cancer Lett. 386 (2017) 189–195.
[10] M.J. Heo, J. Yun, S.G. Kim, Role of non-coding RNAs in liver disease progression to hepatocellular carcinoma, Arch. Pharm. Res (2019).
[11] P. Barman, D. Reddy, S.R. Bhaumik, Mechanisms of antisense transcription initiation with implications in gene expression, genomic integrity and disease pathogenesis, Noncoding RNA 5 (1) (2019).
[12] G. Ors-Kumoglu, S. Gulce-Iz, C. Biray-Avci, Therapeutic microRNAs in human cancer, Cytotechnology (2019).
[13] E. D'Angelo, M. Agostini, Long non-coding RNA and extracellular matrix: the hidden players in cancer-stroma cross-talk, Noncoding RNA Res. 3 (4) (2018) 174–177.
[14] R. Zhang, T. Xia, Long non-coding RNA XIST regulates PDCD4 expression by interacting with miR-21-5p and inhibits osteosarcoma cell growth and metastasis, Int. J. Oncol. 51 (5) (2017) 1460–1470.
[15] Y. Liu, J. Zhang, C. Xing, S. Wei, N. Guo, Y. Wang, miR-486 inhibited osteosarcoma cells invasion and epithelial-mesenchymal transition by targeting PIM1, Cancer Biomark. 23 (2) (2018) 269–277.
[16] R. Jiang, C. Zhang, G. Liu, R. Gu, H. Wu, MicroRNA-126 inhibits proliferation, migration, invasion, and EMT in osteosarcoma by targeting ZEB1, J. Cell. Biochem. 118 (11) (2017) 3765–3774.
[17] Y.B. Wang, Q. Shi, G. Li, J.H. Zheng, J. Lin, W. Qiu, MicroRNA-488 inhibits progression of colorectal cancer via inhibition of the mitogen-activated protein kinase pathway by targeting claudin-2, Am. J. Physiol. Cell Physiol. 316 (1) (2019) C33–C47.
[18] D. Hu, D. Shen, M. Zhang, N. Jiang, F. Sun, S. Yuan, K. Wan, MiR-488 suppresses cell proliferation and invasion by targeting ADAM9 and lncRNA HULC in hepatocellular carcinoma, Am. J. Cancer Res. 7 (10) (2017) 2070–2080.
[19] Y. Zhao, G. Lu, X. Ke, X. Lu, X. Wang, H. Li, M. Ren, S. He, miR-488 acts as a tumor suppressor gene in gastric cancer, Tumour Biol. 37 (7) (2016) 8691–8698.
[20] B. Shi, W. Yan, G. Liu, Y. Guo, MicroRNA-488 inhibits tongue squamous carcinoma cell invasion and EMT by directly targeting ATF3, Cell. Mol. Biol. Lett. 23 (2018) 28.
[21] K.B. Jones, Z. Salah, S. Del Mare, M. Galasso, E. Gaudio, G.J. Nuovo, F. Lovat, K. LeBlanc, J. Palatini, R.L. Randall, S. Volinia, G.S. Stein, C.M. Croce, J.B. Lian, R.I. Aqeilan, miRNA signatures associate with pathogenesis and progression of osteosarcoma, Cancer Res. 72 (7) (2012) 1865–1877.
[22] J. Qiu, Y. Zhang, H. Chen, Z. Guo, MicroRNA-488 inhibits proliferation, invasion and EMT in osteosarcoma cell lines by targeting aquaporin 3, Int. J. Oncol. 53 (4) (2018) 1493–1504.
[23] X. Wei, L. Yu, X. Kong, miR-488 inhibits cell growth and metastasis in renal cell carcinoma by targeting HMGN5, Onco Targets Ther. 11 (2018) 2205–2216.
[24] Y. Xu, W. Wu, Q. Han, Y. Wang, C. Li, P. Zhang, H. Xu, New insights into the interplay between non-coding RNAs and RNA-binding protein HnRNPK in regulating cellular functions, Cells 8 (1) (2019).
[25] U.H. Weidle, F. Birzele, G. Kollmorgen, R. Rüger, Long non-coding RNAs and their role in metastasis, Cancer Genomics Proteomics 14 (3) (2017) 143–160.
[26] C. Zhu, D. Cheng, X. Qiu, M. Zhuang, Z. Liu, Long noncoding RNA SNHG16 promotes cell proliferation by sponging MicroRNA-205 and upregulating ZEB1 expression in osteosarcoma, Cell. Physiol. Biochem. 51 (1) (2018) 429–440.
[27] P. Su, S. Mu, Z. Wang, Long noncoding RNA SNHG16 promotes osteosarcoma cells migration and invasion via sponging miRNA-340, DNA Cell Biol. 38 (2) (2019) 170–175.
[28] Y. Liu, S. Gu, H. Li, J. Wang, C. Wei, Q. Liu, SNHG16 promotes osteosarcoma progression and enhances cisplatin resistance by sponging miR-16 to upregulate ATG4B expression, Biochem. Biophys. Res. Commun. 518 (1) (2019) 127–133.
[29] S. Liao, S. Xing, Y. Ma, LncRNA SNHG16 sponges miR-98-5p to regulate cellular processes in osteosarcoma, Cancer Chemother. Pharmacol. 83 (6) (2019) 1065–1074.
[30] W. Li, S. Zhang, Survival of patients with primary osteosarcoma and lung metastases, J. Buon 23 (5) (2018) 1500–1504.
[31] Y. Wang, J. Yao, H. Meng, Z. Yu, Z. Wang, X. Yuan, H. Chen, A. Wang, A novel long non-coding RNA, hypoxia-inducible factor-2alpha promoter upstream transcript, functions as an inhibitor of osteosarcoma stem cells in vitro, Mol. Med. Rep. 11 (4) (2015) 2534–2540.
[32] D.L. Yu, T. Zhang, K. Wu, Y. Li, J. Wang, J. Chen, X.Q. Li, X.G. Peng, J.N. Wang, L.G. Tan, MicroRNA-448 suppresses metastasis of pancreatic ductal adenocarcinoma through targeting JAK1/STAT3 pathway, Oncol. Rep. 38 (2) (2017) 1075–1082.
[33] Y. Wu, X. Tan, P. Liu, Y. Yang, Y. Huang, X. Liu, X. Meng, B. Yu, M. Wu, H. Jin, ITGA6 and RPSA synergistically promote pancreatic cancer invasion and metastasis via PI3K and MAPK signaling pathways, Exp. Cell Res. 379 (1) (2019) 30–47.
[34] L. Guo, J. Fu, S. Sun, M. Zhu, L. Zhang, H. Niu, Z. Chen, Y. Zhang, L. Guo, S. Wang, MicroRNA-143-3p inhibits colorectal cancer metastases by targeting ITGA6 and ASAP3, Cancer Sci. 110 (2) (2019) 805–816.
[35] Y.P. Jin, Y.P. Hu, X.S. Wu, Y.S. Wu, Y.Y. Ye, H.F. Li, Y.C. Liu, L. Jiang, F.T. Liu, Y.J. Zhang, Y.J. Hao, X.Y. Liu, Y.B. Liu, miR-143-3p targeting of ITGA6 suppresses tumour growth and angiogenesis by downregulating PLGF expression via the PI3K/AKT pathway in gallbladder carcinoma, Cell Death Dis. 9 (2) (2018) 182.
[36] Q. Wen, L. Zhao, T. Wang, N. Lv, X. Cheng, G. Zhang, L. Bai, LncRNA SNHG16 drives proliferation and invasion of papillary thyroid cancer through modulation of miR-497, Onco Targets Ther. 12 (2019) 699–708.
[37] K. Zhang, J. Chen, H. Song, L.-B. Chen, SNHG16/miR-140-5p axis promotes esophagus cancer cell proliferation, migration and EMT formation through regulating ZEB1, Oncotarget 9 (1) (2018) 1028–1040.